*J Physiol* 593.15 (2015) pp 3333–3350



The Journal of Physiology

# The role of $Ca^{2+}$ influx in spontaneous $Ca^{2+}$ wave propagation in interstitial cells of Cajal from the rabbit urethra

Bernard T. Drumm[1,2,3], Roddy J. Large[1], Mark A. Hollywood[1], Keith D. Thornbury[1], Salah A. Baker[3], Brian J. Harvey[2], Noel G. McHale[1] and Gerard P. Sergeant[1]

[1] *Smooth Muscle Research Centre, Dundalk Institute of Technology, Dundalk, Co. Louth, Ireland*
[2] *Department of Molecular Medicine, Royal College of Surgeons in Ireland, Beaumont Hospital, Dublin 9, Ireland*
[3] *Department of Physiology and Cell Biology, University of Nevada School of Medicine, Reno, Nevada, 89557, USA*

**Key points**

- Tonic contractions of rabbit urethra are associated with spontaneous electrical slow waves that are thought to originate in pacemaker cells termed interstitial cells of Cajal (ICC).
- ICC pacemaker activity results from their ability to generate propagating $Ca^{2+}$ waves, although the exact mechanisms of propagation are not understood.
- In this study, we have identified spontaneous localised $Ca^{2+}$ events for the first time in urethral ICC; these were due to $Ca^{2+}$ release from the endoplasmic reticulum (ER) via ryanodine receptors (RyRs) and, while they often remained localised, they sometimes initiated propagating $Ca^{2+}$ waves.
- We show that propagation of $Ca^{2+}$ waves in urethral ICC is critically dependent upon $Ca^{2+}$ influx via reverse mode NCX.
- Our data provide a clearer understanding of the intracellular mechanisms involved in the generation of ICC pacemaker activity.

**Abstract** Interstitial cells of Cajal (ICC) are putative pacemaker cells in the rabbit urethra. Pacemaker activity in ICC results from spontaneous propagating $Ca^{2+}$ waves that are modulated by $[Ca^{2+}]_o$ and whose propagation is inhibited by inositol tri-phosphate receptor ($IP_3R$) blockers. The purpose of this study was to further examine the role of $Ca^{2+}$ influx and $Ca^{2+}$ release in the propagation of $Ca^{2+}$ waves. Intracellular $Ca^{2+}$ was measured in Fluo-4-loaded ICC using a Nipkow spinning disc confocal microscope at fast acquisition rates (50 fps). We identified previously undetected localised $Ca^{2+}$ events originating from ryanodine receptors (RyRs). Inhibiting $Ca^{2+}$ influx by removing $[Ca^{2+}]_o$ or blocking reverse mode sodium–calcium exchange (NCX) with KB-R 7943 or SEA-0400 abolished $Ca^{2+}$ waves, while localised $Ca^{2+}$ events persisted. Stimulating RyRs with 1 mM caffeine restored propagation. Propagation was also inhibited when $Ca^{2+}$ release sites were uncoupled by buffering intracellular $Ca^{2+}$ with EGTA-AM. This was reversed when $Ca^{2+}$ influx via NCX was increased by reducing $[Na^+]_o$ to 13 mM. Low $[Na^+]_o$ also increased the frequency of $Ca^{2+}$ waves and this effect was blocked by tetracaine and ryanodine but not 2-aminoethoxydiphenyl borate (2-APB). RT-PCR revealed that isolated ICC expressed both $RyR_2$ and $RyR_3$ subtypes. We conclude: (i) RyRs are required for the initiation of $Ca^{2+}$ waves, but wave propagation normally depends on activation of $IP_3Rs$; (ii) under resting conditions, propagation by $IP_3Rs$ requires sensitisation by influx of $Ca^{2+}$ via reverse mode NCX; (iii) propagation can be maintained by RyRs if they have been sensitised to $Ca^{2+}$.



DOI: 10.1113/JP270883

(Resubmitted 6 May 2015; accepted after revision 1 June 2015; first published online 5 June 2015)
**Corresponding author** B. T. Drumm: 1664 North Virginia Street, Room 100, Anderson Health Science Building, Department of Physiology and Cell Biology, University of Nevada School of Medicine, Reno, NV, USA. Email: bdrumm@medicine.nevada.edu

**Abbreviations** 2-APB, 2-aminoethyldiphenylborate; AM, acetoxymethyl ester; ANOVA, analysis of variance; CICR, calcium-induced calcium release; ER, endoplasmic reticulum; fps, frames per second; GI, gastrointestinal; ICC, interstitial cells of Cajal; $IP_3$, inositol 1,4,5-triphosphate; NA, numerical aperture; NCX, sodium–calcium exchange; PKA, protein kinase A; PLC, phospholipase C; RyR, ryanodine receptor; SERCA, sarcoplasmic reticulum- ATPase; SMC, smooth muscle cell; STD, spontaneous transient depolarisation; STIC, spontaneous transient inward current; STOC, spontaneous transient outward current; TIFF, tagged image file format.

## Introduction

In mammals, tonic contractions of urethral smooth muscle contribute to urinary continence by preventing leakage of urine from the bladder to the exterior during bladder filling (Brading, 1999). The spontaneous myogenic tone generated by the smooth muscle wall of the urethra is associated with the occurrence of spontaneous electrical slow waves, similar to those observed in the gastrointestinal (GI) tract (Hashitani *et al.* 1996; Hashitani & Edwards, 1999). Slow waves in the GI tract originate in interstitial cells of Cajal (ICC) (Sanders *et al.* 2006) and there is now evidence that a similar pacemaking mechanism exists in the urethra (Sergeant *et al.* 2000). The rabbit urethra contains a sub-population of cells, now referred to as urethral ICC, that are non-contractile, lack myosin, and possess an abundance of vimentin intermediate filaments. These cells are spontaneously active and exhibit regular spontaneous transient depolarisations (STDs) under current-clamp conditions and spontaneous transient inward currents (STICs) under voltage clamp (Sergeant *et al.* 2000). STICs result from the activation of $Ca^{2+}$-activated $Cl^-$ channels by propagating waves of $Ca^{2+}$ released from intracellular $Ca^{2+}$ stores (Sergeant *et al.* 2001). Previous studies have demonstrated that the propagation of these $Ca^{2+}$ waves was critical for STIC activation, since the disruption of $Ca^{2+}$ wave propagation with the inositol 1,4,5-triphosphate receptor ($IP_3R$) blocker 2-aminoethoxydiphenyl-borate (2-APB) inhibited STICs (Johnston *et al.* 2005). Thus, it appears that the ability of ICC in the urethra to fire spontaneous propagating $Ca^{2+}$ waves is fundamental to their role as electrical pacemakers in this tissue (Drumm *et al.* 2014*a*).

$Ca^{2+}$ influx is also vital for the generation of $Ca^{2+}$ waves in urethral ICC (Johnston *et al.* 2005) and subsequent studies indicated that reverse mode sodium–calcium exchange (NCX) was the primary pathway by which this $Ca^{2+}$ influx occurred (Bradley *et al.* 2006; Drumm *et al.* 2014*b*). However, the precise mechanism by which $Ca^{2+}$ influx contributes to spontaneous $Ca^{2+}$ wave propagation in urethral ICC remains unclear.

In the current study, we sought to advance our understanding of the molecular mechanisms underlying spontaneous $Ca^{2+}$ transients in rabbit urethral ICC. We used fast confocal microscopy to examine localised $Ca^{2+}$ events that were previously undetected in prior studies. We sought to specifically evaluate the role played by $Ca^{2+}$ influx and ER $Ca^{2+}$ release channels in the initiation and propagation of $Ca^{2+}$ waves and we propose a new model for $Ca^{2+}$ wave generation and propagation in this cell type. We also performed RT-PCR on isolated smooth muscle cells (SMC) and ICC to investigate which RyR and $IP_3R$ isoforms may be involved in this process.

## Methods

### Ethical approval

All procedures were carried out in accordance with current European Union legislation and with the approval of Dundalk Institute of Technology Animal Use and Care Committee.

### Cell isolation

Male and female New Zealand white rabbits (16–20 weeks old) were humanely killed with a lethal injection of pentobarbitone (I.V.). The mid urethra was removed and placed in Krebs solution and individual SMC and ICC were isolated enzymatically as previously described (Bradley *et al.* 2006).

### Cell selection for RT-PCR

Freshly dispersed cells from rabbit urethra were placed in 35 mm Petri dishes and placed on a Nikon inverted microscope. The isolated cells were allowed to settle to the bottom of the dish for 60 min and cells that remained in suspension were washed away by application of Hank' solution. When a cell was identified on the basis of its morphological characteristics, a large diameter micropipette tip was positioned next to it and negative pressure applied to introduce the cell into the micropipette. Approximately 50 smooth muscle cells (SMC)

and 15 ICC were collected in this way for each RNA preparation.

### Total RNA isolation and RT-PCR

Total RNA was prepared from all tissues using the Trizol method (Invitrogen, Grand Island, NY, USA) and from isolated cells using the Rneasy Micro Kit (Qiagen, Manchester, UK) as per manufacturer's instructions. All RNA samples were DNase treated to remove any contaminating genomic DNA. First-strand cDNA was prepared from the tissue RNA preparations using the Superscript II Reverse Transcriptase kit (Invitrogen), and 200 $\mu$g $\mu$l$^{-1}$ random hexamers were used to reverse transcribe the RNA. For RNA preparations from single cells, first strand synthesis of cDNA was carried out using Sensiscript reverse transcriptase (Invitrogen) with 200 $\mu$g $\mu$l$^{-1}$ random hexamer. The cDNA reverse transcription product was amplified with specific primers by PCR. PCR was performed in a 25-$\mu$l reaction containing Amplitaq Gold PCR Mastermix (Applied Biosystems, Grand Island, NY, USA) as per manufacturer's instructions. All reactions were performed in a Techne TC-512 gradient cycler. The genes were amplified by 35–40 cycles of 95°C for 30 s, 56°C for 30 s, and 72°C for 20 s and, finally, an extension step at 72°C for 10 min. The amplified products were separated by electrophoresis on a 2% agarose–TAE (Tris, acetic acid, EDTA) gel, and the DNA bands were visualised by ethidium bromide staining. The PCR products obtained from RNA isolated from the single- cell preparation were subjected to a second round of amplification and run on a gel. Prior to the second amplification, the PCR product was purified using a QIAquick PCR Purification Kit (Qiagen) with spin column technology as per manufacturers instructions. The details of each primer used in the current study are summarised in Table 1. cDNA derived from the rabbit brain was used as a positive control for the various primers. In all RT-PCR experiments, PCR was also performed on reaction mixtures lacking cDNA for each primer to test for contamination and non-specific amplification; no amplification product was detected from these control experiments (data not shown).

### Calcium imaging

Two millilitres of isolated cell suspension was mixed with 2.0 ml of 100 $\mu$M $Ca^{2+}$ Hanks solution and settled on a glass bottomed dish (WillCo-dish, 22 mm diameter), mounted on the stage of a Nikon Eclipse T*i* microscope and allowed to settle for $\sim$ 30 min at room temperature. Cells were incubated with the acetoxymethyl ester (AM) tagged fluophore Fluo-4 (500 nM final concentration) for 5 min at room temperature. Cells were maintained at 37°C in normal Hanks solution and imaged through a Plan Apo VC (1.4NA) $\times$60 oil immersion lens using an iXon 897 EMCCD camera (Andor Technology, Belfast, UK; 512 $\times$ 512 pixels, pixel size 16 $\times$ 16 $\mu$m) coupled to a Nipkow spinning disk confocal head (CSU22, Yokogawa, Japan; Coates *et al.* 2004). A krypton–argon laser (Melles Griot UK) at 488 nm was used to excite the Fluo-4, and the emitted light was detected at wavelengths $>$ 510 nm. ICC were easily distinguished from SMC on the basis of their distinct morphological characteristics and the lack of contraction in response to 10 mM caffeine.

### Image analysis

Acquisition of recordings was performed on a desktop PC using iQ software (Andor, Belfast, UK). Movie files recorded in iQ were converted to a stack of TIFF (tagged image file format) images and imported into Image J (version1.40, National Institutes of Health, MD, USA, http://rsbweb.nih.gov/ij) for *post hoc* analysis. Prior to analysis, background fluorescence was subtracted from the stack. A single pixel line was drawn along the mid-axis of the cell and using the 'reslice' function in Image J a pseudo linescan image was produced with distance along the cell ($\mu$m) on the vertical axis and time (s) on the horizontal axis. Basal fluorescence was obtained from areas of the cell displaying the most uniform and least intense fluorescence ($F_0$). A colour-coded LUT was then imported into the TIFF to show low intensity fluorescence as cold colours (blue/green) and high intensity fluorescence as warmer colours (yellow/red). To analyse $Ca^{2+}$ waves, a plot profile was first generated, by drawing a rectangle over the entire linescan and plotting an intensity profile in Image J. The amplitude of $Ca^{2+}$ waves was obtained by calculating the difference between basal $Ca^{2+}$ fluorescence and the peak $Ca^{2+}$ fluorescence. Amplitude was expressed as $\Delta F/F_0$. $Ca^{2+}$ waves were defined as events which were $>$ 25% of the maximum amplitude event during a control period. This analysis was used in Figs 7 and 8 where only propagating $Ca^{2+}$ waves were of interest.

In some experiments (Figs 1–4) both $Ca^{2+}$ waves and localised, non-propagating, $Ca^{2+}$ events were analysed. Events were defined as those whose amplitude was $>$ 20% of the maximum intensity event in control conditions. Propagation distance was obtained by thresholding the linescan to 10% of the maximum intensity event during the control period. The spread of the event that remained after threshold was measured on the linescan and taken as the propagation distance. Event spread was not included for those whose amplitude did not reach 20% of the maximum control events. It should be noted that at the speed of acquisition and using a $\times$60 objective, the minimum spread of a $Ca^{2+}$ event that could be detected in this study was 0.27 $\mu$m.

**Table 1. Design of primers used in the current study**

| Primer name | Genbank ID | Position | Sequence (5′ to 3′) | Amplicon |
|---|---|---|---|---|
| Vimentin F | AY465353 | 31–49 | CGTCTTGACCTTGAACGTA | 142 bp |
| Vimentin R | | 155–172 | CAGGCTTGGAAACATCCA | — |
| Smooth muscle myosin F | M77812 | 279–299 | GCTGGTGGAGAATGGGAAGAA | 286 bp |
| Smooth muscle myosin R | | 545–564 | GGCGTAGATGTGTGGTGGCA | — |
| Protein gene product 9.5 F | X04741 | 144–167 | GCTGCTGCTGTTTCCCCTCACGG | 325 bp |
| Protein gene product 9.5 R | | 446–468 | TTGTCATCTACCCGACACTGGCC | — |
| Prolyl-4-hydoxylase F | J05602 | 1201–1218 | GGGGAAGAACTTCGAGGA | 217 bp |
| Prolyl-4-hydoxylase R | | 1400–1417 | GAACTTGAGCGTTGGGAA | — |
| Mast cell carb A F | J05118 | 719–736 | CCAGGAACCAAAACTCCA | 218 bp |
| Mast cell carb A R | | 919–936 | TAGCATCTGCGAGTAGGA | — |
| RYR1 F | X15209 | 8396–8415 | CGTCATCGAGGACTGTCTCA | 238 bp |
| RYR1 R | | 8614–8633 | CCAGAAGAGTTTGCGTGTGA | — |
| RYR2 F | U50465 | 9908–9927 | GCCAATGTGGAAGATGTGTG | 227 bp |
| RYR2 R | | 10115–10134 | TTCATGTGCTCCGAGTTCAG | — |
| RYR3 F | X68650 | 13953–13971 | CTGGTACACAACCATGTCA | 518 bp |
| RYR3 R | | 14453–14470 | CATTGCCAATGCCACAGA | — |
| $IP_3R1$ F | NM_001007235 | 7030–7049 | AGCAAGGCAGCAAGATCAAT | 221 bp |
| $IP_3R1$ R | | 7231–7250 | GTGCGGCTCTAGTGTTCCTC | — |
| $IP_3R2$ F | NM_010586 | 4596–4615 | ATTTGGACAGCCAGGTCAAC | 173 bp |
| $IP_3R2$ R | | 4749–4768 | GGCCACGACATCCTGTAACT | — |
| $IP_3R3$ F | NM_080553 | 7716–7735 | GAGCACATCAAACTGGAGCA | 342 bp |
| $IP_3R3$ R | | 8038–8057 | GCTCATGCAGTTCTGCACAT | — |

F, forward; R, reverse.

In each data set, cells were taken from a minimum of two animals. In describing data, $n = x$ refers to numbers of animals and $c = x$ refers to the numbers of cells tested. Statistical analysis was performed using either Student's paired *t*-test or ANOVA with Tukey's multiple comparison test where appropriate. In all statistical analyses, $P < 0.05$ was taken as significant.

## Solutions

The solutions used were of the following composition (mM):

(1) Krebs Solution: NaCl (120), KCl (5.9), $NaHCO_3$ (25), $NaH_2PO_4.2H_2O$ (1.2), glucose (5.5), $MgCl_2$ (1.2), $CaCl_2$ (2.5). pH was maintained at 7.4 by continuous bubbling of the solution with 95%$O_2$–5% $CO_2$.
(2) $Ca^{2+}$-free Hanks solution (cell isolation): NaCl (125.0), KCl (5.4), glucose (10.0), sucrose (2.9), $NaHCO_3$ (4.2), $KH_2PO_4$ (0.4), $NaH_2PO4$ (0.3), Hepes (10.0) pH to 7.4 using NaOH.
(3) 100$\mu$M $Ca^{2+}$ Hanks solution: $CaCl_2.2H_2O$ (0.1), NaCl (125.0), KCl (5.4), glucose (10.0), sucrose (2.9), $NaHCO_3$ (4.2), $KH_2PO_4$ (0.4), $NaH_2PO_4$ (0.3), Hepes (10.0). pH to 7.4 using NaOH.
(4) $Ca^{2+}$-free Hanks solution (superfusion): NaCl (125.0), KCl (5.4), glucose (10.0), sucrose (2.9), $NaHCO_3$ (4.2), $KH_2PO_4$ (0.4), $NaH_2PO_4$ (0.3), $MgCl_2.6H_2O$ (2.3), EGTA (5.0), $MgSO_4$ (0.4), Hepes (10.0). pH to 7.4 using NaOH.
(5) Hanks solution: NaCl (125.0), KCl (5.4), glucose (10.0), sucrose (2.9), $NaHCO_3$ (4.2), $KH_2PO_4$ (0.4), $NaH_2PO_4$ (0.3), $MgCl_2.6H_2O$ (0.5), $CaCl_2.2H_2O$ (1.8), $MgSO_4$ (0.4), Hepes (10.0). pH to 7.4 using NaOH.
(6) 13 mM $Na^+$ Hanks solution: NMDG (117 mM) NaCl (8), KCl (5.4), glucose (10.0), sucrose (2.9), $NaHCO_3$ (4.2), $KH_2PO_4$ (0.4), $NaH_2PO_4$ (0.3), $MgCl_2.6H_2O$ (0.5), $CaCl_2.2H_2O$ (1.8), $MgSO_4$ (0.4), Hepes (10.0). pH to 7.4 using HCl.

## Drugs

Drugs used were: EGTA-AM, ryanodine and KB-R 7943 from Tocris, Abingdon, UK, tetracaine and caffeine from Sigma, Wicklow, Ireland 2-aminoethoxydiphenyl borate (2-APB) from Acros, Geel, Belgium and SEA-0400 (HY-15515) from MedChemtronica, Stockholm, Sweden Drugs were made up in DMSO (EGTA-AM, KB-R 7943, ryanodine, SEA-0400), ethanol (2-APB) or water (tetracaine) depending on solubility, note that caffeine was directly dissolved to its final concentration in Hanks solution or $Ca^{2+}$-free Hanks solution.

The cell under study was continuously superfused with Hanks solution by means of a close delivery system consisting of a pipette (tip diameter 200 $\mu$m) placed

approximately 300 $\mu$m away. This could be switched, with a dead-space time of ~5 s, to a solution containing a drug. All experiments were carried out at 35–37°C.

## Results

### Urethral ICC exhibit a wide range of $Ca^{2+}$ events

As reported in previous studies (Johnston *et al.* 2005; Sergeant *et al.* 2006*a*,*b*, 2008; Bradley *et al.* 2010; Drumm *et al.* 2014*b*,*c*), only $Ca^{2+}$ waves could be adequately resolved in isolated rabbit urethral ICC at low image acquisition rates (5–15 fps). A typical example of such a recording is shown in Fig. 1*A*, where it is clear that ICC exhibited regular propagating $Ca^{2+}$ waves, which could traverse the entire length of the cell. However, the relatively low acquisition rates used in these previous studies may have been insufficient to detect brief, localised transient $Ca^{2+}$ events that can occur at the ER. In many cell types, a localised $Ca^{2+}$ signal may provide a 'trigger' for $Ca^{2+}$ waves, for example $Ca^{2+}$ sparks in cardiac cells (Cheng *et al.* 1993) and $Ca^{2+}$ puffs in *Xenopus* oocytes (Yao & Parker, 1994). Therefore, in the current study, isolated ICC were imaged using a fast acquisition rate (50–97 fps) to examine the underlying $Ca^{2+}$ events.

At faster acquisition rates (50 fps), a range of localised $Ca^{2+}$ events were identified in different ICC, as illustrated

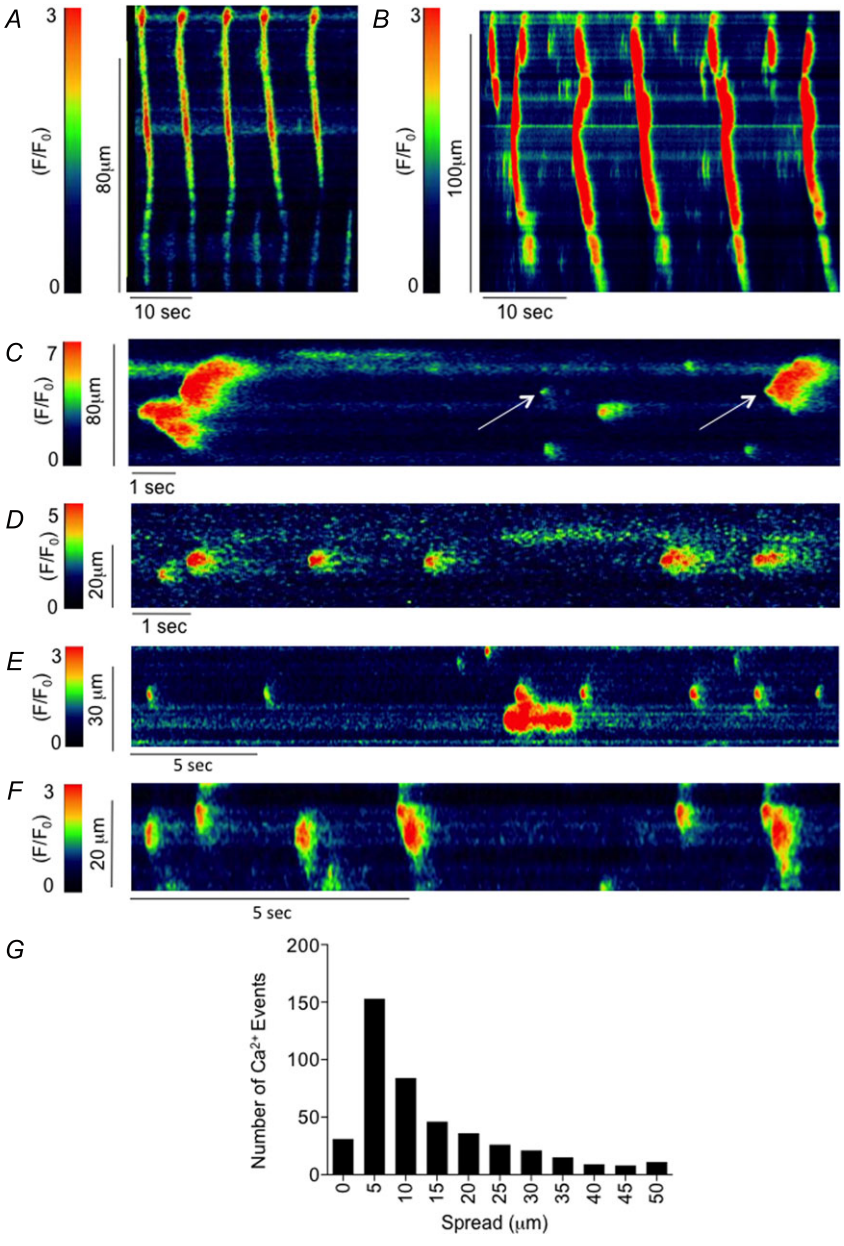


**Figure 1. ICC display spontaneous $Ca^{2+}$ events of varying spread**
*A*, 5 fps recording of spontaneous $Ca^{2+}$ waves in an isolated rabbit urethral ICC. *B*, at 50 fps both $Ca^{2+}$ waves and localised events can also be observed in ICC. *C–F*, range of spontaneous $Ca^{2+}$ events in different ICC observed using fast acquisition rates (50 fps). As well as propagating $Ca^{2+}$ waves, ICC also fired spontaneous $Ca^{2+}$ events that had a localised spread. Limitations of recording at 5 fps meant that these localised events could be undetected, thus fast frame rates (50 fps) were required to observe these events. *G*, histogram showing the range and distribution of $Ca^{2+}$ signal propagation spread in ICC. In order to achieve frame rates of 50 fps, the size of the recording chip needed to be cropped and this degree of cropping could vary from cell to cell. Thus, in the case of some cells, we could only record 50 $\mu$m of cell length and others were over 100 $\mu$m, and a histogram of spread measurements would be skewed to the left as it would not be possible to fill the bins greater than 50 $\mu$m accurately. Thus, in the histogram shown, the maximum bin is the shortest cell length that could be recorded from (50 $\mu$m). A total of 32 $Ca^{2+}$ events were measured in other cells that propagated greater than 50 $\mu$m, the maximum of which was 178.8 $\mu$m. The spread of $Ca^{2+}$ events shown are binned into 5 $\mu$m increments ($n = 9$, $c = 16$).

in Fig. 1*B*–*G*. These $Ca^{2+}$ events displayed variable spatial properties. For example, in Fig. 1*C* a localised transient $Ca^{2+}$ event (indicated by the first white arrow) can be seen firing near the mid-point of the linescan and spread ~2.5 $\mu$m. A few seconds later another event occurred at the same site, but this event propagated ~40 $\mu$m. Although this event was not as localised as the first event, it did not propagate the entire cell length and thus could be described as an 'intermediate' event or 'attenuated' $Ca^{2+}$ wave. Thus, it can be seen that ICC exhibit a continuum of $Ca^{2+}$ transients ranging from discrete localised events (Fig. 1*D*–*F*), to $Ca^{2+}$ waves, which can propagate along the entire cell length (Fig. 1*A* and *B)* with a range of 'intermediate' events in between (Fig. 1*B* and *C)*. From 472 events measured in 16 different ICC ($n = 9$) recorded at 50 fps, the spatial spread of $Ca^{2+}$ transients ranged from 1.1 $\mu$m to 178.8 $\mu$m (Fig. 1*G*).

## The effect of blocking $Ca^{2+}$ influx in ICC

$Ca^{2+}$ waves in urethral ICC can be abolished by $Ca^{2+}$-free solutions (Johnston *et al.* 2005). However, the low acquisition rates (5 fps) employed in this study precluded investigation of brief, localised $Ca^{2+}$ events. We therefore sought to investigate if localised $Ca^{2+}$ events occurred in ICC when $Ca^{2+}$ influx was impaired.

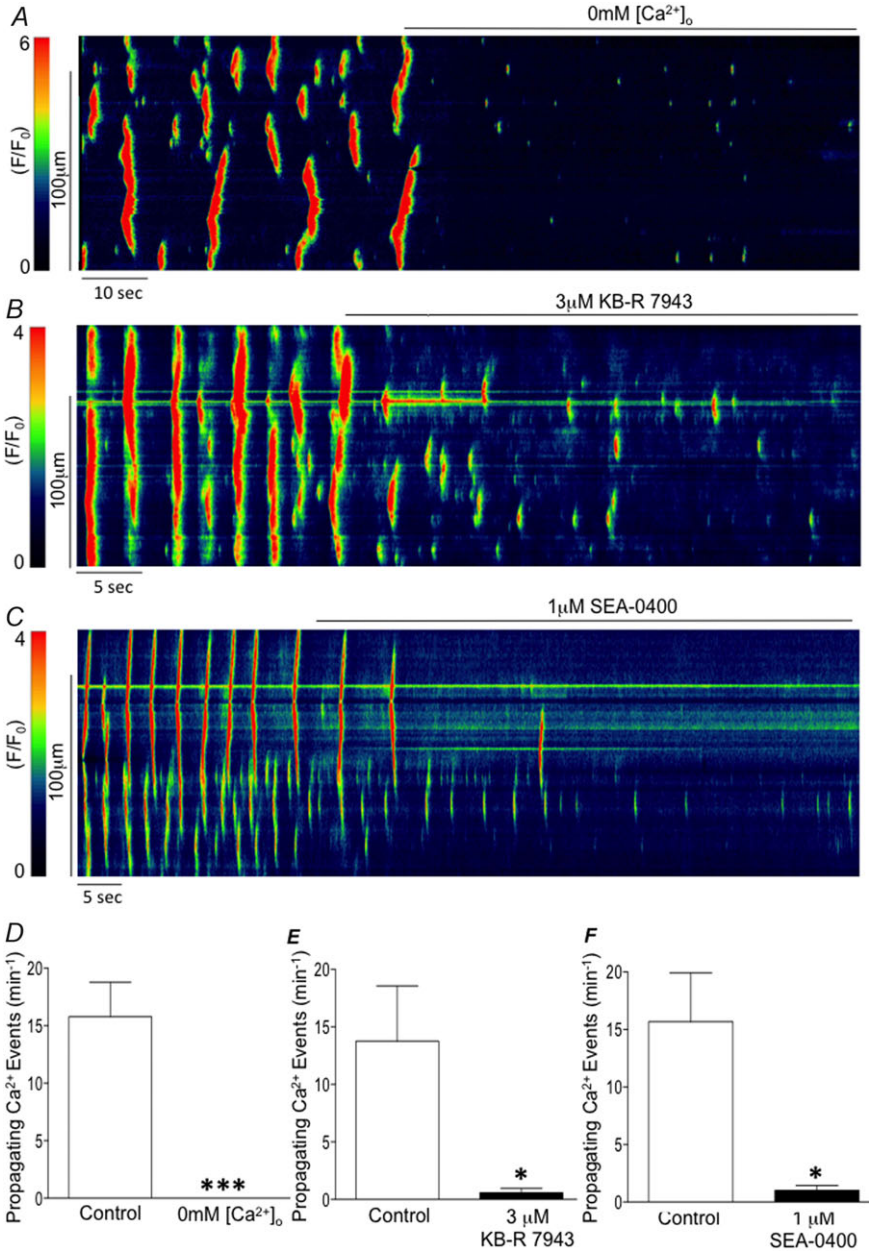


**Figure 2. The effect of blocking $Ca^{2+}$ influx on $Ca^{2+}$ events**
*A*, representative line scan recorded at 50 fps showing the effect of zero $[Ca^{2+}]_o$ on $Ca^{2+}$ wave propagation and initiation. *B*, representative line scan recorded at 50 fps showing the effect of blocking NCX with 3 $\mu$M KB-R 7943 on $Ca^{2+}$ wave propagation and initiation. *C*, representative line scan recorded at 50 fps showing the effect of blocking NCX with 1 $\mu$M SEA-0400 on $Ca^{2+}$ wave propagation and initiation. *D*, summary data showing the frequency of propagating $Ca^{2+}$ events (>25 $\mu$m) during a control period compared with 0 mM $[Ca^{2+}]_o$ conditions (***$P < 0.0004$, paired *t* test, $n = 8$, $c = 11$). *E*, summary data showing the frequency of propagating $Ca^{2+}$ events (>25 $\mu$m) during a control period compared with 3 $\mu$M KB-R 7943 conditions (*$P < 0.03$, paired *t* test, $n = 3$, $= 6$). *F*, summary data showing the frequency of propagating $Ca^{2+}$ events (>25 $\mu$m) during a control period compared with 1 $\mu$M SEA-0400 conditions (*$P < 0.02$, paired *t* test, $n = 3$, $n = 6$).

Under control $[Ca^{2+}]_o$ (1.8 mM), ICC exhibited a range of $Ca^{2+}$ transients of varying spread (Fig. 2*A*). Upon removal of extracellular $Ca^{2+}$, the propagating $Ca^{2+}$ waves were abolished; however, localised $Ca^{2+}$ events persisted (Fig. 2*A*). Propagating $Ca^{2+}$ events were defined as those events that spread more than 25$\mu$m. The summary data in Fig. 2*D* show that the frequency of propagating $Ca^{2+}$ events in control conditions was $15.8 \pm 3$ min$^{-1}$ and these were abolished in $Ca^{2+}$-free conditions (Fig. 2*D*, $P < 0.001$, paired *t* test, $n = 8$, $c = 11$).

Reverse mode sodium–calcium exchange (NCX) is believed to act as the main $Ca^{2+}$ influx pathway in ICC (Bradley *et al.* 2006; Drumm *et al.* 2014*b*). When $Ca^{2+}$ influx was blocked with the specific reverse mode NCX blocker KB-R 7943 (3 $\mu$M, Fig. 2*B*), or SEA-0400 (1 $\mu$M, Fig. 2*C*), $Ca^{2+}$ wave propagation was reduced, but localised events remained. There was a significant difference in the frequency of propagating $Ca^{2+}$ events before ($13.75 \pm 4.8$ min$^{-1}$) and during KB-R 7943 application ($0.58 \pm 0.37$ min$^{-1}$, Fig. 2*E*, $P < 0.03$, paired *t* test, $n = 3$, $c = 6$). Similarly, application of SEA-0400 (Fig. 2*F*) reduced propagating event frequency from $15.67 \pm 4.2$ min$^{-1}$ to $1 \pm 0.44$ min$^{-1}$ ($P < 0.02$, paired *t* test, $n = 3$, $c = 6$).

These data suggested that $Ca^{2+}$ influx, via reverse NCX, was essential for $Ca^{2+}$ wave propagation, possibly by sensitising ER $Ca^{2+}$ release channels. If this were the case, one would expect that increasing the sensitivity of the ER $Ca^{2+}$ release channels in the absence of $Ca^{2+}$ influx should restore $Ca^{2+}$ propagation activity. That this is the case is demonstrated in Fig. 3, which shows that application of a low concentration of caffeine (1 mM) to ICC treated with $Ca^{2+}$-free Hanks solution induced a series of propagating $Ca^{2+}$ waves. The summary data in Fig. 3*B* indicate that 1 mM caffeine induced a series of propagating $Ca^{2+}$ events with a mean frequency of $6.8 \pm 2$ min$^{-1}$, whereas prior to addition of caffeine no propagating events were observed ($P < 0.013$, paired *t* test, $n = 5$, $c = 7$).

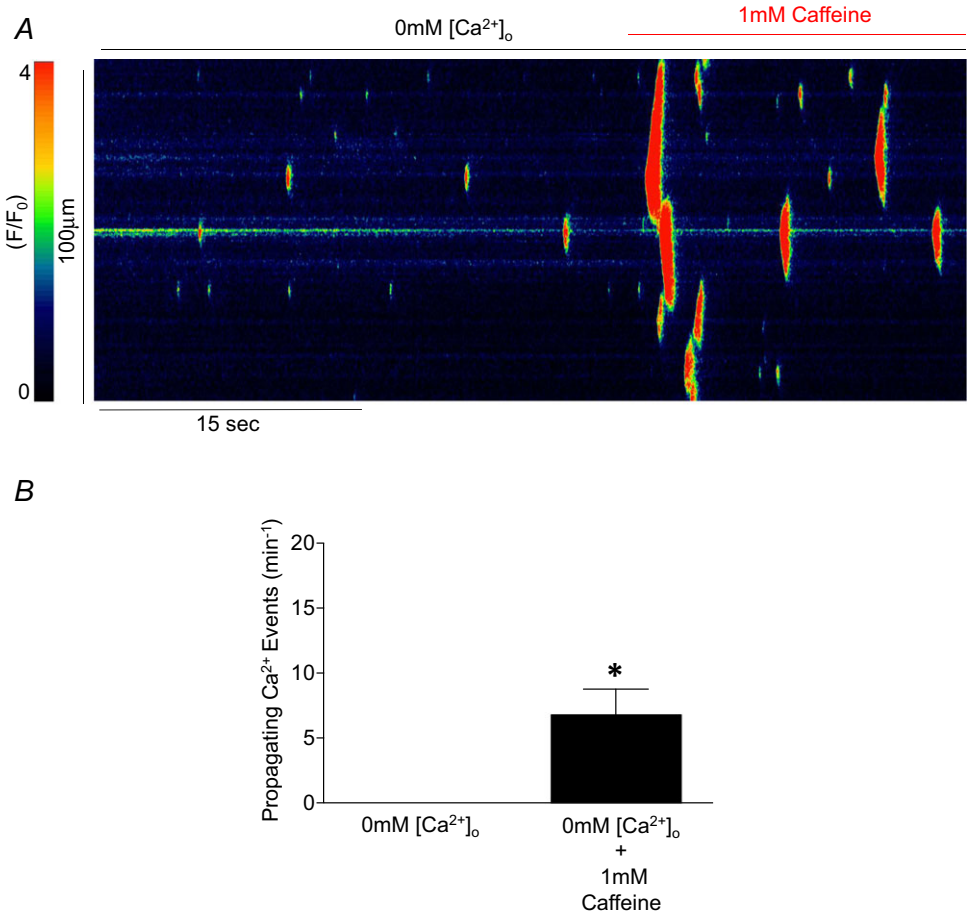


**Figure 3. 1 mm caffeine increases the spread of $Ca^{2+}$ events in $Ca^{2+}$-free conditions**
*A*, representative line scan recorded at 50 fps showing the effect of 1 mM caffeine on $Ca^{2+}$ events in zero $[Ca^{2+}]_o$. *B*, summary data showing the frequency of propagating $Ca^{2+}$ events (>25 $\mu$m) during 0 mM $[Ca^{2+}]_o$ conditions compared with 0 mM $[Ca^{2+}]_o$ conditions in the presence of 1 mM caffeine (*$P < 0.013$, paired *t* test, $n = 5$, $c = 7$).

### The effect of EGTA-AM on $Ca^{2+}$ events

$Ca^{2+}$ release from the ER and its diffusion to neighbouring sites of release appeared to be essential for the propagation of $Ca^{2+}$ waves. We tested this propagation mechanism further by applying EGTA-AM (a slow $Ca^{2+}$ chelator), which we speculated would inhibit the propagation of $Ca^{2+}$ waves, but unmask the primary $Ca^{2+}$ events responsible for initiating the $Ca^{2+}$ waves. This expected result was observed in all experiments with EGTA ($n = 6$, $c = 10$) and an example is shown in Fig. 4*A* and *B*. Thus, in the absence of EGTA-AM the spatial spread of $Ca^{2+}$ events ranged from 1.1 to 178.8 $\mu$m ($n = 9$, $c = 16$), whereas in EGTA-AM the range was much narrower (1.1 to 29 $\mu$m, $n = 6$, $c = 10$). Next we investigated if the localised $Ca^{2+}$ events, which remained in the presence of EGTA, could be converted to propagating $Ca^{2+}$ waves by enhancing $Ca^{2+}$ influx. This was achieved by reducing $[Na^+]_o$ from 130 mM to 13 mM to drive reverse mode NCX (Bradley *et al.* 2006). The representative trace in Fig. 4*D* indicates that application of 13 mM $[Na^+]_o$, in the continued presence of EGTA-AM, restored propagating $Ca^{2+}$ waves. In five similar experiments, the frequency of propagating events increased from 0.6 ± 0.6 $min^{-1}$ in EGTA-AM to 7.12 ± 1.12 $min^{-1}$ in the presence of EGTA-AM plus 13 mM $[Na^+]_o$ (Fig. 4*E*, $P < 0.0017$, paired *t* test, $n = 2$, $c = 5$).

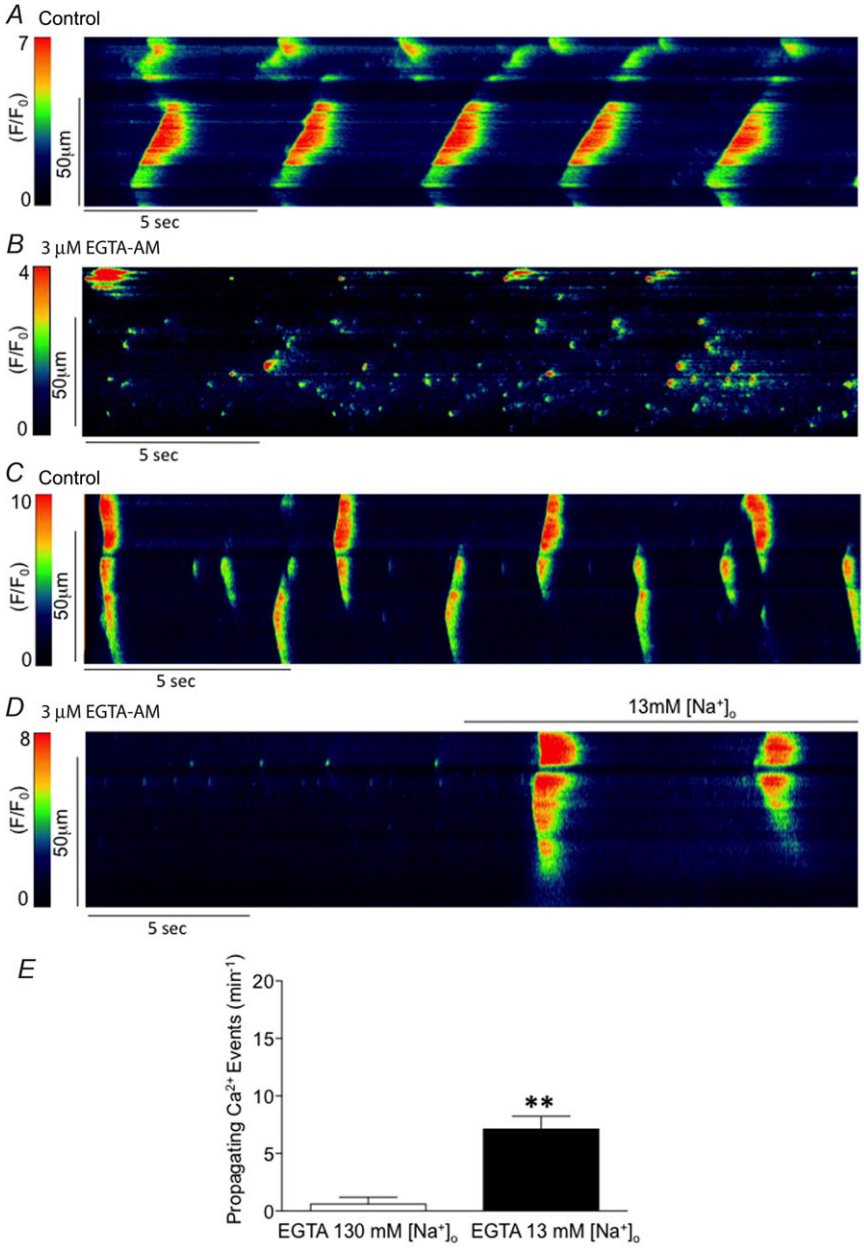


**Figure 4. The effect of EGTA-AM on $Ca^{2+}$ events**
*A* and *C*, representative linescan recorded at 50 fps showing an ICC firing propagating $Ca^{2+}$ waves. *B*, after 40 minutes incubation with the slow acting $Ca^{2+}$ chelator EGTA-AM (3 $\mu$M), $Ca^{2+}$ waves were abolished and only localised $Ca^{2+}$ events remained intact. *D*, upon lowering $[Na^+]_o$ from 130 mM to 13 mM, localised events in EGTA-AM were converted into propagating $Ca^{2+}$ waves. *E*, summary data showing the frequency of propagating $Ca^{2+}$ events (>25 $\mu$m) during EGTA-AM conditions compared with EGTA-AM conditions with 13 mM $Na^+$ ($P < 0.0017$, paired *t* test, $n = 2$, $c = 5$).

### $IP_3Rs$ are required for $Ca^{2+}$ wave propagation but not initiation

Previous studies on urethral ICC showed that blocking RyR-mediated $Ca^{2+}$ release from the ER, with tetracaine or ryanodine, abolished STICs and $Ca^{2+}$ oscillations. In contrast, $IP_3R$ blockade with 2-APB decreased $Ca^{2+}$ wave propagation and reduced STIC amplitude, but not frequency (Johnston *et al.* 2005). This suggested that $IP_3Rs$ were involved in the propagation of $Ca^{2+}$ waves, but not their initiation. We investigated this idea further by examining the effect of tetracaine and 2-APB at higher acquisition rates than used previously. We observed that all $Ca^{2+}$ activity was abolished in ICC imaged at 97 fps using the RyR blocker tetracaine (Fig. 5*A*). However, at the same acquisition rate, inhibition of $IP_3Rs$ with 2-APB only blocked $Ca^{2+}$ wave propagation but localised $Ca^{2+}$ events remained (Fig. 5*B*). Interestingly, it was apparent from this example that, under control conditions, the cell produced a localised event, which itself did not lead to a propagating $Ca^{2+}$ wave, but seemed to trigger a neighbouring site to fire a $Ca^{2+}$ wave. In the presence of 2-APB localised $Ca^{2+}$ events remained at the site of localised $Ca^{2+}$ wave initiation (Fig. 5*C* and *D*), whereas in the presence of tetracaine all $Ca^{2+}$ events were abolished (Fig. 5*A*).

Several studies have indicated that, in addition to inhibiting $IP_3Rs$, 2-APB may also have non-specific effects on store-operated $Ca^{2+}$ entry, sarcoplasmic reticulum-ATPase (SERCA) pumps and RyR-mediated $Ca^{2+}$ release (Iwasaki *et al.* 2001; Putney, 2001; Bootman *et al.* 2002; Peppiatt *et al.* 2003). In order to examine the selectivity of 2-APB we examined its effect on phenylephrine- and caffeine-evoked $Ca^{2+}$ transients, to stimulate $Ca^{2+}$ release from $IP_3Rs$ and RyRs, respectively. The representative traces in Fig. 6*A* and *B* indicate that phenylephrine-induced $Ca^{2+}$ oscillations were greatly diminished in the presence of 2-APB, whereas 10 mM caffeine-induced responses remained intact. This experiment was representative of 6 others, summarised in Fig. 6*D*, which shows that 100 $\mu$M 2-APB significantly reduced the phenylephrine (1 $\mu$M) response ($P < 0.008$, paired $t$ test). On the other hand caffeine responses, were only slightly reduced in amplitude and this effect was not statistically significant (NS, paired $t$ test, $n = 2$, $c = 6$). The slight reduction is likely due to a rundown of the 10 mM caffeine response as similar observations were made in control experiments in the absence of 2-APB (Supporting Fig. S1). Therefore these data suggest that 2-APB selectively affected the $IP_3$-dependent response and did not affect the refilling or release from ryanodine-sensitive $Ca^{2+}$ stores. Experiments were also performed with the phospholipase C inhibitor U73122 (10 $\mu$M). However, in contrast to 2-APB, U73122

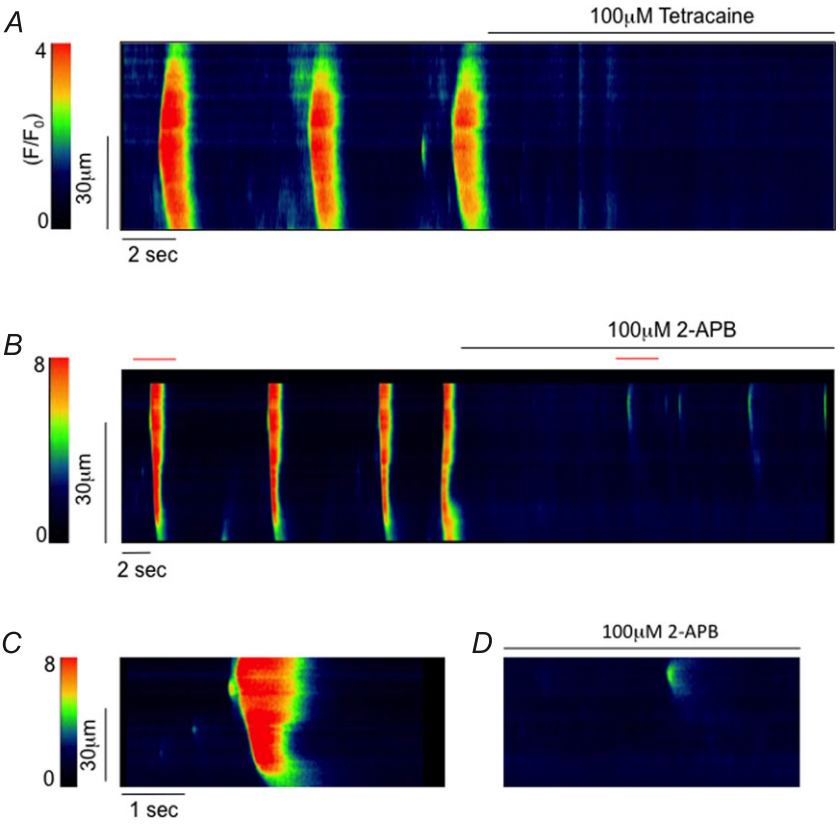


**Figure 5. Localised $Ca^{2+}$ events arise from the ER via RyR-mediated release**
*A*, representative linescan recorded at 97 fps showing that inhibition of RyRs with 100 $\mu$M tetracaine abolished all $Ca^{2+}$ activity in ICC including localised $Ca^{2+}$ signals. *B*, representative linescan recorded at 97 fps showing that inhibition of $IP_3Rs$ with 100 $\mu$M 2-APB inhibited the propagation of $Ca^{2+}$ waves in ICC but did not prevent the firing of initial localised $Ca^{2+}$ events. The highlighted events on the linescan were enlarged and put on an expanded timescale in *C* and *D*. At these expanded time scales it was clear that 2-APB did not block the initial localised $Ca^{2+}$ events that preceded $Ca^{2+}$ waves.

significantly inhibited 10 mM caffeine responses in ICC and also significantly increased basal $Ca^{2+}$ (Supporting Fig. S2), suggesting that it may block SERCA pumps, as has been reported by Olson *et al.* (2010).

The data gathered in this study thus far suggest that $Ca^{2+}$ waves are initiated by localised $Ca^{2+}$ events, at RyRs, which are converted to $Ca^{2+}$ waves if neighbouring $IP_3Rs$ are adequately sensitised by $Ca^{2+}$ influx.

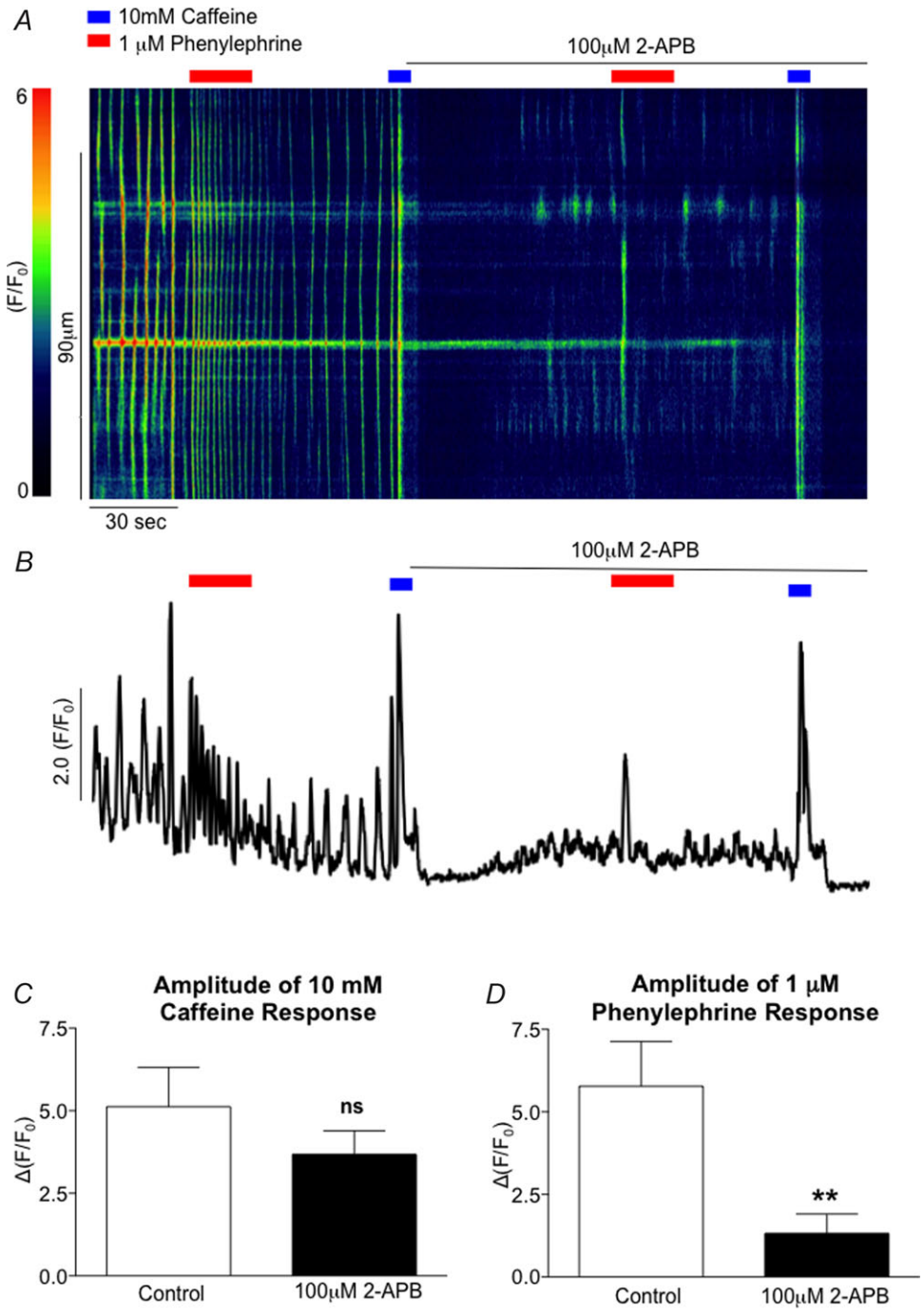


**Figure 6. The effect of 2-APB on ER $Ca^{2+}$ store load and RyR-mediated release**
*A*, representative linescan recorded at 5 fps showing the effect of 100 $\mu$M 2-APB on the amplitude of 10 mM caffeine- and 1 $\mu$M phenylephrine-induced $Ca^{2+}$ transients. *B*, associated plot profile of the linescan shown in panel *A*. *C*, summary data showing the effect of 100 $\mu$M 2-APB on the amplitude of 10 mM caffeine-induced $Ca^{2+}$ transients. *D*, summary data showing the effect of 100 $\mu$M 2-APB on the amplitude of 1 $\mu$M phenylephrine-induced $Ca^{2+}$ transients (**$P < 0.01$, $n = 2$, $c = 6$).

### The effect of 2-APB on $Ca^{2+}$ wave propagation

We next examined if increased $Ca^{2+}$ influx could compensate for reduced $IP_3R$-mediated $Ca^{2+}$ release by examining the effect of 13 mM $[Na^+]_o$ before and during the presence of 2-APB. Figure 7*A* indicates that application of 13 mM $[Na^+]_o$ increased $Ca^{2+}$ wave frequency in urethral ICC and similar responses were observed in the presence of 2-APB, albeit with a reduced amplitude. For example in six cells, low $Na^+$ increased wave frequency from 8.2 ± 1.7 $min^{-1}$ to 14.4 ± 1.9 $min^{-1}$ ($P < 0.05$, ANOVA, Fig. 7*B*, $n = 2$, $c = 6$). In the presence of 2-APB, the frequency of spontaneous $Ca^{2+}$ waves was reduced to 0.25 ± 0.25 $min^{-1}$; however, re-application of low $Na^+$ increased wave frequency to 9.2 ± 2.4 $min^{-1}$ ($P < 0.01$, ANOVA, Fig. 7*B*, $n = 2$, $c = 6$). Application of 2-APB also reduced wave amplitude from 1.1 ± 0.3 to 0.2 ± 0.2 $\Delta F/F_0$ ($P < 0.001$, ANOVA, Fig. 7*C*). Re-application of 13 mM $[Na^+]_o$ in the presence of 2-APB, partially restored mean amplitude to 0.7 ± 0.2 $\Delta F/F_0$ ($P < 0.01$ ANOVA, Fig. 7*C*, $n = 2$, $c = 6$). Control experiments, performed to ensure that the 13 mM $[Na^+]_o$ effects were reproducible, showed that there was no significant difference in the frequency (19 ± 4.5 *vs.* 16.16 ± 3.28 $min^{-1}$, $P < 0.14$, $n = 2$, $c = 4$) or amplitude (0.8 ± 1.4 *vs.* 0.6 ± 0.09 $\Delta F/F_0$, $P < 0.15$, $n = 4$) of $Ca^{2+}$ waves with consecutive application of low Na, in the absence of drugs.

### The effect of RyR inhibition on $Ca^{2+}$ wave propagation

The data above indicate that enhanced $Ca^{2+}$ influx, via reverse mode NCX, could compensate for reduced $IP_3R$-mediated $Ca^{2+}$ release and thus restore propagating

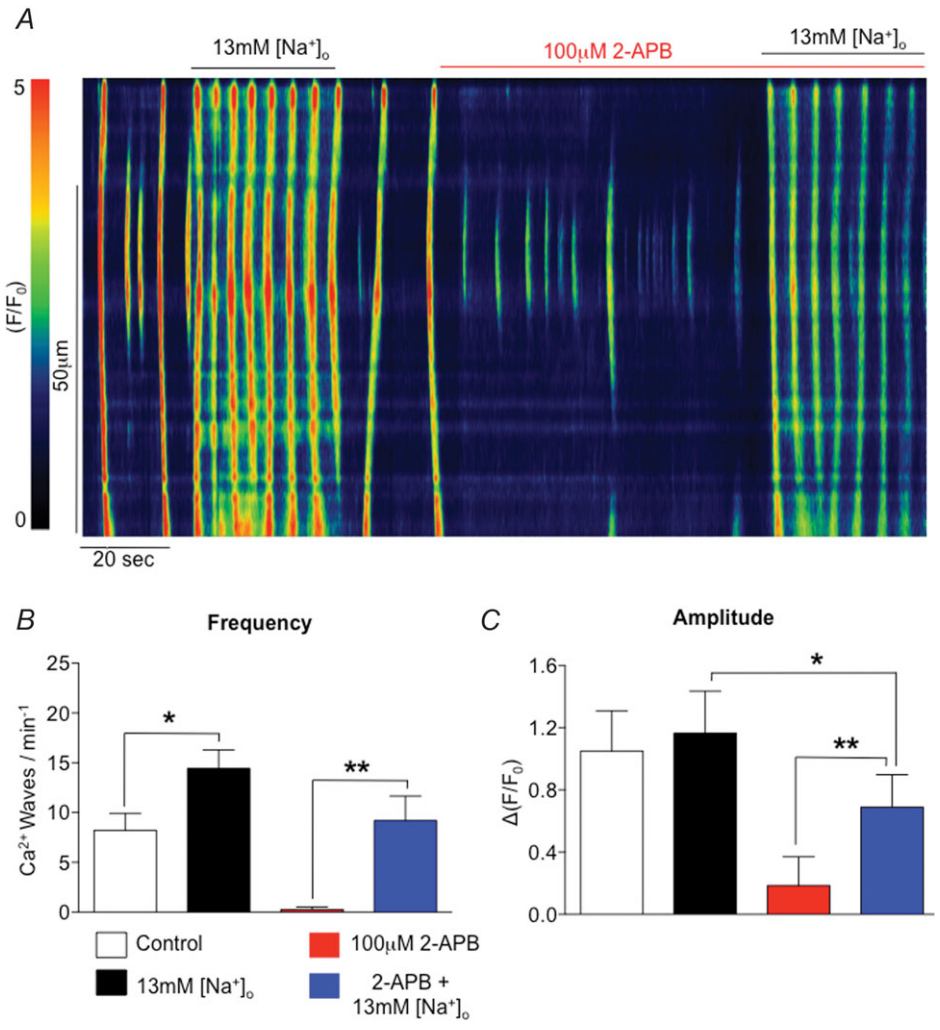


**Figure 7. The effect of blocking $IP_3Rs$ on the effect of 13 mm $Na^+$**
*A*, representative linescan showing the effect of 100 $\mu$M 2-APB on $Ca^{2+}$ waves in the presence of 13 mM $Na^+$. *B* and *C*, summarised data showing the effect of 100 $\mu$M 2-APB on $Ca^{2+}$ wave frequency and amplitude in the presence of 13 mM $Na^+$ (*$P < 0.05$, **$P < 0.01$, $n = 2$, $c = 6$).

$Ca^{2+}$ waves. Next, we examined if similar results could be achieved when RyRs were blocked. However, as Fig. 8 suggests, enhanced $Ca^{2+}$ influx, via reverse NCX did not restore $Ca^{2+}$ waves when $Ca^{2+}$ release via RyRs was reduced, with either tetracaine or ryanodine. In 10 cells, 13 mM $[Na^+]_o$ increased wave frequency from 8.7 ± 1.7 to 14.7 ± 1 $min^{-1}$ ($P < 0.01$, ANOVA, Fig. 8*C*, $n = 3$). $Ca^{2+}$ waves were significantly inhibited by application of 100 $\mu$M tetracaine $Ca^{2+}$ (0.4 ± 0.2 $min^{-1}$, $P < 0.001$, ANOVA, Fig. 8*C*, $n = 3$, $c = 10$). Re-application of 13 mM $[Na^+]_o$, in the presence of tetracaine, failed to restore $Ca^{2+}$ wave frequency (1.6 ± 0.6 $min^{-1}$, $P < 0.001$, ANOVA, $n = 3$). Similarly, application of 30 $\mu$M ryanodine abolished $Ca^{2+}$ waves (Fig. 8*B*) and these were not restored

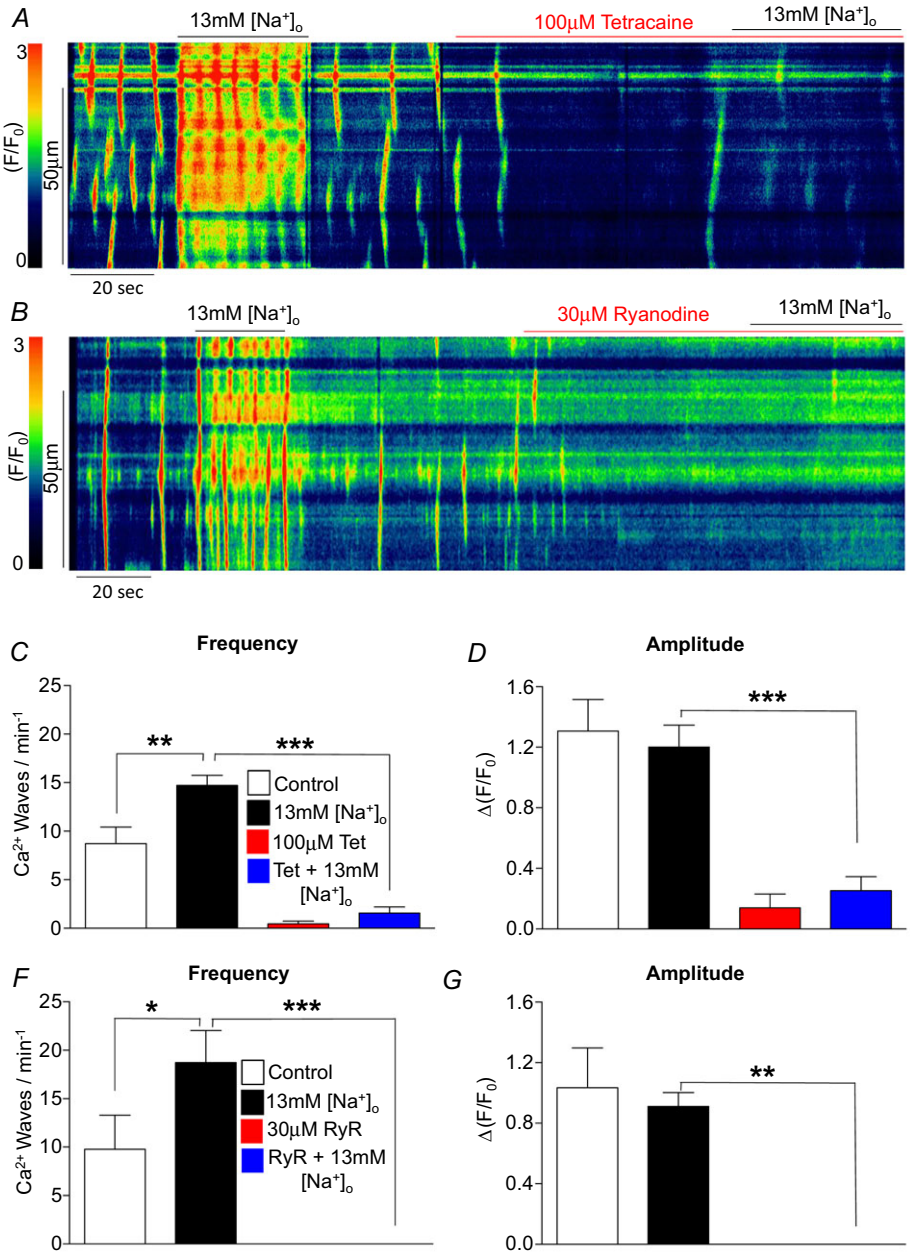


**Figure 8. The effect of blocking RyRs on the effect of 13 mm $Na^+$**
*A*, representative linescan recorded at 15 fps showing the effect of 100 $\mu$M tetracaine on $Ca^{2+}$ waves in the presence of 13 mM $Na^+$. *B*, representative linescan recorded at 5 fps showing the effect of 30 $\mu$M ryanodine on $Ca^{2+}$ waves in the presence of 13 mM $Na^+$. *C* and *D*, summarised data showing the effect of 100 $\mu$M tetracaine on $Ca^{2+}$ wave frequency and amplitude in the presence of 13 mM $Na^+$ (**$P < 0.01$, ***$P < 0.001$, $n = 3$, $c = 10$). *F* and *G*, summarised data showing the effect of 30 $\mu$M ryanodine on $Ca^{2+}$ wave frequency and amplitude in the presence of 13 mM $Na^+$ (*$P < 0.05$, **$P < 0.01$, ***$P < 0.001$, $n = 2$, $c = 5$).

in 13 mM $[Na^+]_o$ (Fig. 8*F* and *G* $n = 2$, $c = 5$). These data suggest that RyRs are crucial for the generation of $Ca^{2+}$ waves, such that increased $Ca^{2+}$ influx cannot compensate for the inhibitory effects of RyR blockade.

### Expression of RyR and $IP_3R$ subtypes in rabbit urethra

The data presented thus far indicate that $Ca^{2+}$ waves in urethral ICC are dependent upon release of $Ca^{2+}$ from both RyRs and $IP_3$Rs and $Ca^{2+}$ influx via reverse mode NCX. A previous study indicated that urethral ICC specifically expressed NCX3 and not NCX1 and NCX2, (Bradley *et al.* 2006); however, the molecular identity of the RyRs and $IP_3$Rs involved in this activity have not been elucidated. Therefore, we performed RT-PCR experiments to examine the expression of these isoforms in isolated rabbit urethral ICC, isolated urethral smooth muscle cells and whole urethral smooth muscle strips.

In order to confirm the identity of the collected cells, control experiments were performed to examine the transcriptional expression of specific markers for different cell types. For example, the intermediate filament vimentin was used to identify interstitial cells, smooth muscle myosin (SMMY) was used as a marker for SMC, protein gene product 9.5 (PGP 9.5) was used as a neuronal maker, prolyl-4-hydroxylase (P4H) for fibroblasts and mast cell carboxypeptidase A for mast cells. Figure 9*A* shows that urethral smooth muscle (SM) strips showed expression of all markers (Fig. 9*Aa*). In contrast, isolated ICC only showed expression for vimentin (Fig. 9*Ab*) and SMC showed expression of smooth muscle myosin only (Fig. 9*Ab*).

Figure 9*B* shows that RYR1-3 were expressed in urethral SM strips (Fig. 9*Ba*), whereas only RyR2 and RyR3 were detected in isolated urethral ICC (Fig. 9*Bb*). Isolated urethral smooth muscle cells, expressed RyR1 and RyR2 (Fig. 9*Bc*). All three $IP_3$R isoforms were detected in urethral SM strips, as shown in Fig. 9*Ca*, however, only expression of $IP_3$R1 and $IP_3$R2 was detected in isolated urethral ICC and SMC (Fig. 9*Cb* and *c*).

## Discussion

Interstitial cells of Cajal act as electrical pacemakers in the urethra by generating spontaneous transient depolarisations that lead to contraction in electrically coupled smooth muscle cells. Previous studies have shown that the electrical pacemaking activity of ICC is dependent on underlying spontaneous intracellular $Ca^{2+}$ waves (Johnston *et al.* 2005; Sergeant *et al.* 2006*b*). Studies conducted in the past have resolved these $Ca^{2+}$ waves using confocal microscopy at slow acquisition rates of 5–15 fps and no localised $Ca^{2+}$ events were detected (Johnston *et al.* 2005; Sergeant *et al.* 2006*a*,*b*, 2008; Bradley *et al.* 2010; Drumm *et al.* 2014*b*,*c*). In the current study, using confocal microscopy with fast acquisition rates (50 fps), we observed a range of $Ca^{2+}$ events that have not been reported previously in this cell type. We identified localised $Ca^{2+}$ transients with spatial properties similar to $Ca^{2+}$ sparks or $Ca^{2+}$ puffs, intermediate $Ca^{2+}$ waves and propagating $Ca^{2+}$ waves. Thus, it seems that spontaneous $Ca^{2+}$ signals in ICC, rather than being quantal in nature as reported by Yao *et al.* (1995) in *Xenopus* oocytes, actually occupy a continuum, from highly localised $Ca^{2+}$ events to $Ca^{2+}$ events that can propagate over much greater distances.

Localised $Ca^{2+}$ events persisted in $Ca^{2+}$-free external solution and when $Ca^{2+}$ influx was blocked pharmacologically with the reverse NCX inhibitors KBR-7943 and SEA-0400. Therefore it appears that $Ca^{2+}$ influx, via reverse mode NCX is required for the conversion of localised events to propagating $Ca^{2+}$ waves, but is not essential for their initial generation. These data are consistent with findings in other cell types, including *Xenopus* oocytes (Yao & Parker, 1994), smooth muscle cells (Mironneau *et al.* 1996; Bolton & Gordienko, 1998; 2001; ZhuGe *et al.* 1999; Tumelty *et al.* 2007; McCloskey *et al.* 2009) and cardiac cells (Cheng *et al.* 1993), which demonstrated that $Ca^{2+}$ puffs or $Ca^{2+}$ sparks persist in zero $[Ca^{2+}]_o$ or when $Ca^{2+}$ influx was blocked pharmacologically.

Intracellular $[Ca^{2+}]$ is highly buffered in living cells and increasing cytosolic $Ca^{2+}$ buffering can shape the amplitude and duration of $Ca^{2+}$ signals (Wagner & Keizer, 1994; Berridge *et al.* 2000; Ouyang *et al.* 2005). Buffers such as EGTA and EDTA have been used to uncouple $Ca^{2+}$ release sites and prevent $Ca^{2+}$ wave propagation in *Xenopus* oocytes (Callamaras & Parker, 2000; Marchant & Parker, 2001), cardiac cells (Smith *et al.* 1998; Lukyanenko & Gyorke, 1999) and smooth muscle cells (Olson *et al.* 2010). This protocol was employed in the current study to uncouple $Ca^{2+}$ release sites in urethral ICC using EGTA-AM. In the presence of EGTA-AM, only localised $Ca^{2+}$ events were observed. However, enhanced $Ca^{2+}$ influx via reverse mode NCX restored propagating $Ca^{2+}$ waves in EGTA-AM.

It is possible that raising cytosolic $Ca^{2+}$ levels via increased $Ca^{2+}$ influx may promote $Ca^{2+}$ wave propagation by sensitising $Ca^{2+}$ release channels on the ER, such that they become activated by $Ca^{2+}$ released from a localised event. In this way, increased $Ca^{2+}$ influx may lower the threshold for activation of release channels by increasing their sensitivity to $Ca^{2+}$. Alternatively, the threshold for reaching activation may remain the same and increasing influx may simply increase cytosolic $Ca^{2+}$ sufficiently so that smaller $Ca^{2+}$ events are now able to induce larger propagating events. This has also been suggested in the GI tract; in this tissue $Ca^{2+}$ influx in ICC is believed to occur through a $Ni^{2+}$- and mibefradil-sensitive pathway and leads to increased $[Ca^{2+}]_i$ and increased open

probability of $IP_3Rs$ (Ward *et al.* 2004; Bayguinov *et al.* 2007).

An alternative possibility is that increased luminal ER $Ca^{2+}$ content, resulting from $Ca^{2+}$ influx, may have also increased the sensitivity of ER $Ca^{2+}$ channels to cytoplasmic $Ca^{2+}$ activation. In cardiac cells, ER $Ca^{2+}$ content has been proposed to be involved in $Ca^{2+}$ release by sensitising the release channels to cytosolic $Ca^{2+}$ activation and increasing the open probability of RyRs (Cheng *et al.* 1993; Gyorke & Gyorke, 1998). Computer simulations of cardiac myocytes have found that SR $Ca^{2+}$ release can only occur when luminal $Ca^{2+}$ reaches a certain threshold (Keizer *et al.* 1998). In cardiac myocytes it was shown by Terentyev *et al.* (2002) that while SR depletion inhibited sparks this was overcome by raising cytosolic $Ca^{2+}$. Thus, cytosolic $Ca^{2+}$ levels and not luminal $Ca^{2+}$ content was the major determinant of $Ca^{2+}$ release channel sensitisation. Experiments in toad skeletal muscle also demonstrated that increased SR $Ca^{2+}$ content only marginally increased the frequency of $Ca^{2+}$ sparks and did not induce $Ca^{2+}$ waves (Launikonis *et al.* 2006).

We hypothesised that $Ca^{2+}$ influx sensitised the ER $Ca^{2+}$ release channels to activate in response to localised $Ca^{2+}$ transients by acting on the cytoplasmic side of the channels. In urethral ICC, $Ca^{2+}$-free solutions abolished $Ca^{2+}$ waves and yet under these conditions the $Ca^{2+}$ transient response to 10 mM caffeine responses, which is a measure of ER $Ca^{2+}$ content, remained intact (Johnston *et al.* 2005). This observation indicates that ER $Ca^{2+}$ stores were not rapidly depleted by the removal of $Ca^{2+}$ from the external bathing solution. Therefore, it seems logical that $Ca^{2+}$ influx acts on the cytoplasmic side of the $Ca^{2+}$ release channels on the ER to sensitise their activation to localised $Ca^{2+}$ transients. If $Ca^{2+}$ influx increased receptor sensitisation by increasing luminal $Ca^{2+}$ content one would expect the store to be depleted when waves

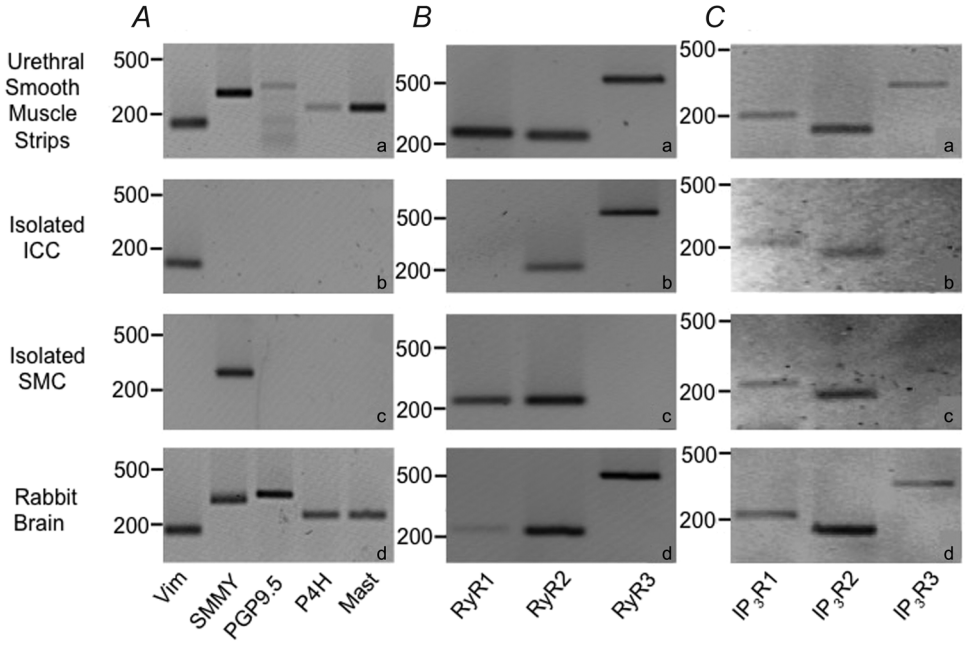


**Figure 9. Expression of RyR and $IP_3R$ isoforms in the rabbit urethra**
*A*, transcriptional expression of cell specific markers in whole tissue and single cell sample from the rabbit urethra. Markers investigated were the intermediate filament vimentin, smooth muscle myosin (SMMY), protein gene product 9.5 (PGP 9.5 – neuronal maker), prolyl-4-hydroxylase (P4H – fibroblast marker) and mast cell carboxypeptidase A (Mast – mast cell marker). RNA was isolated from urethral smooth muscle (SM) strips (*a*) isolated ICC (*b*) and isolated SMC (*c*). As a positive control for primer specificity rabbit brain was included (*d*). Primers were designed to amplify genes whose expression is associated with particular cell types, including vimentin (ICC), smooth muscle myosin (SMC), protein gene product 9.5 (neurons), prolyl-4-hydroxylase (fibroblasts) and mast cell carboxypeptidase A (CPA3, mast cells). The PCR products were separated on a 2% agarose–TAE gel and visualised under UV conditions following ethidium bromide staining. *B*, RT-PCR examination for RyR1, RyR2 and RyR3. Expression profiles of RyR isoforms are shown for urethral smooth muscle strips (*a*), isolated ICC (*b*) and isolated SMCs (*c*). cDNA from rabbit brain was also examined as a positive control for primer specificity (*d*). The PCR amplicons were separated on a 2% agarose–TAE gel and visualised under UV conditions following ethidium bromide staining. *C*, RT-PCR detection of the three $IP_3R$ isoforms using gene specific primers. Template cDNA from urethral muscle strips (*a*), isolated ICC (*b*) and isolated SMCs (*c*) was examined. cDNA from rabbit brain was also examined as a positive control for primer specificity (*d*). The PCR amplicons were separated on a 2% agarose–TAE gel and visualised under UV conditions following ethidium bromide staining.

were abolished in $Ca^{2+}$-free conditions but this is not the case (Johnston *et al.* 2005). Another possible action of increased $Ca^{2+}$ influx may be to increase the levels of $Ca^{2+}$-sensitive PLC, leading to elevated $[IP_3]_i$ (Hisamitsu *et al.* 2001) and this could also lead to greater sensitisation of $IP_3$Rs. However, there is currently no information on this possible PLC signalling mechanism occurring in ICC and this requires further investigation.

In the current study, sensitising the ER $Ca^{2+}$ release channels with low concentrations of caffeine in the absence of $[Ca^{2+}]_o$ led to an increased propagation of $Ca^{2+}$ signals. Caffeine lowers the activation threshold for RyRs by increasing their sensitivity to $Ca^{2+}$ and this mechanism presumably allows localised $Ca^{2+}$ events to activate neighbouring sites at lower $Ca^{2+}$ concentrations than would be possible in control conditions. This RyR sensitisation mechanism is consistent with findings in toad and rat myocytes (Gollasch *et al.* 1998; ZhuGe *et al.* 2004) where increasing RyR sensitivity with low doses of caffeine led to increased $Ca^{2+}$ spark frequency, amplitude and spread. The localised $Ca^{2+}$ events observed in the current study are likely to arise from RyR-mediated release and not from $IP_3$Rs and thus could be labelled $Ca^{2+}$ 'sparks' similar to other RyR-mediated localised $Ca^{2+}$ events in cardiac and smooth muscle cells. This conclusion is supported by our observation that blocking RyRs with tetracaine abolished all $Ca^{2+}$ events but blocking $IP_3$Rs with 2-APB only arrested the $Ca^{2+}$ waves, leaving localised $Ca^{2+}$ events intact.

The specificity of 2-APB has been questioned in a number of studies and has been shown to inhibit RyRs, block SERCA pumps and block store-operated $Ca^{2+}$ entry in several cell types (Iwasaki *et al.* 2001; Putney, 2001; Bootman *et al.* 2002; Peppiatt *et al.* 2003). However, we have several reasons for believing that these reported non-specific effects of 2-APB do not account for its inhibitory effects observed in the present study. Firstly, 2-APB at 100 $\mu$M has been shown to selectively block STICs in urethral ICC but not spontaneous transient outward currents (STOCs), suggesting that it did not affect RyRs or BK channels (Sergeant *et al.* 2001). Secondly, 100 $\mu$M 2-APB did not block caffeine-evoked $Cl^-$ currents in urethral ICC but did block $IP_3$-generated $Cl^-$ currents evoked by noradrenaline (Sergeant *et al.* 2001). Therefore, these data indicated that 2-APB selectively inhibited $IP_3$-dependent responses and also that it did not affect $Ca^{2+}$ -activated $Cl^-$ channels. This was further investigated in the current study. We demonstrated that 2-APB blocked $Ca^{2+}$ transients induced by phenylephrine but not caffeine. Therefore, these data indicate that 2-APB does not affect RyRs or the pathways that are responsible for refilling of ER stores. Furthermore, although 2-APB has been reported to block store-operated $Ca^{2+}$ entry, such an explanation appears unlikely in the current study since Bradley *et al.* 2005 showed that 2-APB was a poor blocker of store-operated $Ca^{2+}$ entry in urethral ICC and that pacemaker activity in these cells was not dependent on this $Ca^{2+}$ entry pathway (Bradley *et al.* 2005). Taken together with the results of the present study, these findings suggest that the inhibitory effects of 2-APB in the present study were mediated by an effect on $IP_3$Rs.

Our observations are also consistent with previous studies in which RyR blockers abolished STICs in ICC, while $IP_3$Rs inhibitors reduced in STIC amplitude rather than frequency (Johnston *et al.* 2005). The data in the present study suggest that the localised $Ca^{2+}$ transients were due to $Ca^{2+}$ release from the ER via RyRs and that these events were converted to $Ca^{2+}$ waves by regenerative $Ca^{2+}$ release from $IP_3$Rs. These $Ca^{2+}$ waves could then propagate along the cell and activate sufficient numbers of $Ca^{2+}$-activated $Cl^-$ channels on the plasma membrane to elicit STICs of large enough amplitude needed to generate electrical pacemaking activity.

It is clear that $IP_3$Rs are involved in the propagation of $Ca^{2+}$ waves in urethral ICC. However, low $[Na^+]_o$ restored propagating $Ca^{2+}$ waves when $IP_3$Rs were blocked with 2-APB, but not when RyRs were inhibited. This suggests, that RyRs were capable of generating propagating $Ca^{2+}$ waves if $Ca^{2+}$ influx was enhanced. A similar model was suggested in *Xenopus* oocytes by Dupont & Goldbeter (1994). This 'two pool' model, stated that under control conditions both $IP_3$ and $Ca^{2+}$ were required for

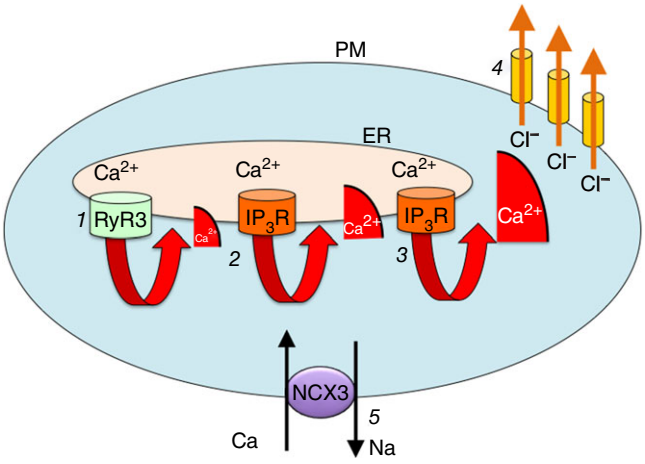


**Figure 10. ICC $Ca^{2+}$ wave initiation and propagation**
1, $Ca^{2+}$ waves originate from an initial localised release of $Ca^{2+}$ from the ER via RyRs, possibly from the RyR3 subtype. 2, $Ca^{2+}$ from the initial release diffuses to a neighbouring cluster of $IP_3$Rs and activates them via CICR. 3, activation of the $IP_3$Rs clusters leads to regenerative $Ca^{2+}$ release from the ER and results in a propagating $Ca^{2+}$ wave. 4, the $Ca^{2+}$ wave activates chloride channels on the plasma membrane, leading to the generation of pacemaker STICs (spontaneous transient inward currents). 5, the regenerative release of $Ca^{2+}$ from $IP_3$Rs requires that the receptors be adequately sensitised to activate, this is accomplished via $Ca^{2+}$ influx through the reverse mode NCX3 isoform.

propagating $Ca^{2+}$ waves; however $Ca^{2+}$ waves could occur in the absence of $IP_3$ if $Ca^{2+}$ influx was raised sufficiently to sensitise the $IP_3$Rs to participate in regenerative $Ca^{2+}$ release. This is as opposed to a 'single pool' model in which both $IP_3$ and $Ca^{2+}$ were absolutely required for $Ca^{2+}$ wave propagation. In urethral ICC, we propose a 'three pool model' consisting of RyRs, $IP_3$Rs and $Ca^{2+}$ (influx). $Ca^{2+}$ release from RyRs is an absolute requirement in all cases to provide the initial $Ca^{2+}$ wave signal, while under normal conditions $IP_3$ and $Ca^{2+}$ act as co-agonists that sensitise the $IP_3$R, and thus facilitate $Ca^{2+}$ wave propagation. However, in the absence of functional $IP_3$Rs, $Ca^{2+}$ waves can still occur if RyRs are sensitised to the extent that they become functionally coupled. These ideas are summarised in Fig. 10.

The results of the present study show that urethral ICC expressed both RyR2 and RyR3 isoforms, whereas isolated urethral smooth muscle cells only expressed RyR1 and RyR2. On the other hand both cell types expressed both $IP_3$R1 and $IP_3$R2 isoforms, but not $IP_3$R3. Therefore it is tempting to speculate that the $Ca^{2+}$ events, underlying pacemaker activity in ICC, could be associated with expression of RyR3, as this isoform was exclusively expressed in ICC. This finding is also in agreement with studies by Aoyama *et al.* (2004) and Liu *et al.* (2005*a*), which demonstrated that RyR3 was expressed in ICC from the small intestine and stomach.

In conclusion, this study demonstrates that urethral ICC exhibit an array of $Ca^{2+}$ events ranging from highly localised $Ca^{2+}$ events to propagating $Ca^{2+}$ waves. $Ca^{2+}$ waves were converted to localised $Ca^{2+}$ events by 2-APB and reverse mode NCX inhibitors, suggesting that propagating $Ca^{2+}$ waves rely on both $Ca^{2+}$ release from $IP_3$Rs and $Ca^{2+}$ influx via reverse mode NCX. Application of tetracaine and ryanodine inhibited all $Ca^{2+}$ oscillations, suggesting that they are responsible for the generation of localised $Ca^{2+}$ events that may initiate $Ca^{2+}$ waves. These results confirm our previous inference that calcium oscillations in isolated rabbit urethral ICC are initiated by calcium release from RyRs, which may therefore be considered as the primary oscillator, and that conversion of the primary oscillation to a propagated calcium wave depends upon $IP_3$-induced calcium release. It now appears that this process is facilitated by $Ca^{2+}$ influx via reverse NCX, which may prime the $IP_3$Rs, such that they respond to $Ca^{2+}$ release from RyRs. These data give us a clearer understanding of the intracellular pathways that underlie ICC $Ca^{2+}$ pacemaker activity and may provide insights into the mechanisms responsible for the generation of urethral tone. This could be of significance in the future development of therapeutic actions to counter urinary incontinence.

## References


Aoyama M, Yamada A, Wang J, Ohya S, Furuzono S, Goto T, Hotta S, Ito Y, Matsubara T, Shimokata K *et al.* (2004). Requirement of ryanodine receptors for pacemaker $Ca^{2+}$ activity in ICC and HEK293 cells. *J Cell Sci* **117**, 2813–2825.

Bayguinov PO, Ward SM, Kenyon JM & Sanders KM (2007). Voltage-gated $Ca^{2+}$ currents are necessary for slow wave propagation in the canine gastric antrum. *Am J Physiol Cell Physiol* **293**, C1645–C1659.

Berridge MJ, Lipp P & Bootman MD (2000). The versatility and universality of calcium signalling. *Nat Rev Mol Cell Biol* **1**, 11–21.

Boittin FX, Macrez N, Halet G & Mironneau J (1999). Norepinephrine-induced $Ca^{2+}$ waves depend on $InsP_3$ and ryanodine receptor activation in vascular myocytes. *Am J Physiol Cell Physiol* **277**, C139–C151.

Bolton TB & Gordienko DV (1998). Confocal imaging of calcium release events in single smooth muscle cells. *Acta Physiol Scand* **164**, 567–575.

Bootman MD, Collins TJ, Mackenzie L, Roderick HL, Berridge MJ & Peppiatt CM (2002). 2-Aminoethoxydiphenyl borate (2-APB) is a reliable blocker of store-operated $Ca^{2+}$ entry but an inconsistent inhibitor of $InsP_3$-induced $Ca^{2+}$ release. *FASEB J* **16**, 1145–1150.

Brading AF (1999). The physiology of the mammalian urinary outflow tract. *Exp Physiol* **84**, 215–221.

Bradley JE, Hollywood MA, Johnston L, Large RJ, Matsuda T, Baba A, McHale NG, Thornbury KD & Sergeant GP (2006). Contribution of reverse $Na^+$–$Ca^{2+}$ exchange to spontaneous activity in interstitial cells of Cajal in the rabbit urethra. *J Physiol* **574**, 651–661.

Bradley JE, Hollywood MA, McHale NG, Thornbury KD & Sergeant GP (2005). Pacemaker activity in urethral interstitial cells is not dependent on capacitative calcium entry. *Am J Physiol Cell Physiol* **289**, C625–C632.

Bradley JE, Kadima S, Drumm BT, Hollywood MA, Thornbury KD, McHale NG & Sergeant GP (2010). Novel excitatory effects of adenosine triphosphate on contractile and pacemaker activity in rabbit urethral smooth muscle. *J Urol* **183**, 801–811.

Callamaras N & Parker I (2000). Phasic characteristic of elementary $Ca^{2+}$ release sites underlies quantal responses to $IP_3$. *EMBO* **19**, 3608–3617.

Cheng H, Lederer WJ & Cannell M (1993). Calcium sparks: Elementary events underlying excitation–contraction coupling in heart muscle. *Science* **262**, 740–744.

Cheng H, Lederer MR, Lederer WJ & Cannell M (1996). Calcium sparks and $[Ca^{2+}]_i$ waves in cardiac myocytes. *Am J Physiol Cell Physiol* **270**, C148–C159.

Coates CG, Denvir DJ, McHale NG, Thornbury KD, Hollywood MA (2004). Optimizing low-light microscopy with back-illuminated electron multiplying charge-coupled device: enhanced sensitivity, speed, and resolution. *J Biomed Opt* **9**, 1244–1252.

Coombes S, Hinch R & Timofeeva Y (2004). Receptors, sparks and waves in a fire-diffuse-fire framework for calcium release. *Prog Biophys Mol Biol* **85**, 197–216.

Drumm BT, Koh SD, Andersson KE & Ward SM (2014*a*) Calcium signalling in Cajal-like interstitial cells of the lower urinary tract. *Nat Rev Urol* **11**, 555–564.

Drumm BT, Sergeant GP, Hollywood MA, Thornbury KD, Matsuda T, Baba A, Harvey BJ & McHale NG (2014*b*). The effect of high $[K^+]_o$ on spontaneous $Ca^{2+}$ waves in freshly isolated interstitial cells of Cajal from the rabbit urethra. *Physiol Rep* **2**, e00203, doi: 10.1002/phy2.203

Drumm BT, Sergeant GP, Hollywood MA, Thornbury KD, McHale NG & Harvey BJ (2014*c*). The role of cAMP dependent protein kinase in modulating spontaneous intracellular $Ca^{2+}$ waves in interstitial cells of Cajal from the rabbit urethra. *Cell Calcium* **56**, 181–187.

Dupont G & Goldbeter A (1994). Properties of intracellular $Ca^{2+}$ waves generated by a model based on $Ca^{2+}$ induced $Ca^{2+}$ release. *Biophys J* **67**, 2191–2204.

Gollasch M, Wellman GC, Knot HJ, Jagger J, Damon DH, Bonev AD, Nelson MT (1998). Ontogeny of local sarcoplasmic reticulum $Ca^{2+}$ signals in cerebral arteries. *Circ Res* **83**, 1104–1114.

Gordienko DV, Greenwood IA & Bolton TB (2001). Direct visualization of sarcoplasmic reticulum regions discharging $Ca^{2+}$ sparks in vascular myocytes. *Cell Calcium* **29**, 13–28.

Gyorke I & Gyorke S (1998). Regulation of the cardiac ryanodine receptor channel by luminal $Ca^{2+}$ involves luminal $Ca^{2+}$ sensing sites. *Biophys J* **75**, 2801–2810.

Harhun M, Gordienko D, Kryshtal D, Pucovsky V & Bolton T (2006). Role of intracellular stores in the regulation of rhythmical $[Ca^{2+}]_i$ changes in interstitial cells of Cajal from the rabbit portal vein. *Cell Calcium* **40**, 287–298.

Hashitani H & Edwards FR (1999). Spontaneous and neurally activated depolarizations in smooth muscle cells of the guinea-pig urethra. *J Physiol* **514**, 459–470.

Hashitani H, Lang RJ & Suzuki H (2010). Role of perinuclear mitochondria in the spatiotemporal dynamics of spontaneous $Ca^{2+}$ waves in interstitial cells of Cajal-like cells of the rabbit urethra. *Br J Pharmacol* **161**, 680–694.

Hasitani H, Van Helden DF & Suzuki H (1996). Properties of spontaneous depolarizations in circular smooth muscle cells of rabbit urethra. *Br J Pharmacol* **118**, 1627–1632.

Hisamitsu T, Ohata H, Kawanishi T, Iwamoto T, Shigekawa M, Amano H, Yamada S & Momose K (2001). A mechanism of $Ca^{2+}$ release from $Ca^{2+}$ stores coupling to the $Na^+/Ca^{2+}$ exchanger in cultured smooth muscle cells. *Life Sci* **69**, 2775–2787.

Iwasaki H, Mori Y, Hara Y, Uchida K, Zhou H & Mikoshiba K (2001). 2-Aminoethoxydiphenyl borate (2-APB) inhibits capacitive calcium entry independently of the function of inositol 1,4,5-trisphosphate receptors. *Receptors Channels* **7**, 429–439.

Johnston L, Sergeant GP, Hollywood MA, Thornbury KD & McHale NG (2005). Calcium oscillations in interstitial cells of the rabbit urethra. *J Physiol* **565**, 449–61.

Keizer JE, Smith GD, Ponce-Dawson S & Pearson J (1998). Saltatory propagation of $Ca^{2+}$ waves by $Ca^{2+}$ sparks. *Biophys J* **75**, 595–600.

Launikonis BS, Zhou J, Santiago D, Brum G & Rios E (2006). The changes in $Ca^{2+}$ sparks associated with measured modifications of intra-store $Ca^{2+}$ concentration in skeletal muscle. *J Gen Physiol* **128**, 45–54.

Liu HN, Ohya S, Furuzono J, Imaizumi Y & Nakayama S (2005). Co-contribution of $IP_3$Rs and $Ca^{2+}$ influx pathways to pacemaker $Ca^{2+}$ activity in stomach ICC. *J Biol Rhythms* **20**, 15–26.

Liu HN, Ohya S, Wang J, Imaizumi Y & Nakayama S (2005). Involvement of ryanodine receptors in pacemaking $Ca^{2+}$ oscillations in murine gastric ICC. *Biochem Biophys Res Commun* **328**, 640–646.

Lowie BJ, Wang XY, White EJ & Huizinga JD (2011). On the origin of the rhythmic calcium transients in the ICC-MP of the mouse small intestine. *Am J Physiol Gastrointest Liver Physiol* **301**, G835–G845.

Lukyanenko V & Gyorke S (1999). $Ca^{2+}$ sparks and $Ca^{2+}$ waves in saponin-permeabilised rat ventricular myocytes. *J Physiol* **521**, 575–585.

McCloskey C, Cagney V, Large RJ, Hollywood MA, Sergeant GP, McHale NG & Thornbury KD (2009). Voltage-dependent $Ca^{2+}$ currents contribute to spontaneous $Ca^{2+}$ waves in rabbit corpus cavernosum myocytes. *J Sex Med* **6**, 3019–3031.

Marchant JS & Parker I (2001). Role of elementary $Ca^{2+}$ puffs in generating repetitive $Ca^{2+}$ oscillations. *EMBO* **20**, 65–76.

Mironneau J, Arnaudeau S, Macrez-Lepretre N & Boittin FX (1996). $Ca^{2+}$ sparks and $Ca^{2+}$ waves activate different $Ca^{2+}$-dependent ion channels in single myocytes from rate portal vein. *Cell Calcium* **20**, 153–160.

Olson ML, Chalmers S & McCarron JG (2010). Mitochondrial $Ca^{2+}$ uptake increases $Ca^{2+}$ release from inositol 1,4,5-triphosphate receptor clusters in smooth muscle cells. *Am Soc Biochem Mol Biol* **285**, 2040–2050.

Ouyang K, Wu C & Cheng H (2005). $Ca^{2+}$ induced $Ca^{2+}$ release in sensory neurons. *J Biol Chem* **280**, 15898–15902.

Peppiatt CM, Collins TJ, Mackenzie L, Conway SJ, Holmes AB, Bootman MD, Berridge MJ, Seo JT & Roderick HL (2003). 2-Aminoethoxydiphenylborate (2-APB) antagonizes inositol 1,4,5-triphosphate-induced calcium release, inhibits calcium pumps and has a use dependent and slowly reversible action on store operated calcium entry. *Cell Calcium* **34**, 97–108.

Putney JW (2001). Pharmacology of capacitative calcium entry. *Mol Interv* **1**, 84–94.

Sanders KM & Ward SM (2006). Interstitial cells of Cajal – a new perspective on smooth muscle function. *J Physiol* **576**, 721–726.

Sergeant GP, Bradley JE, Thornbury KD, McHale NG & Hollywood MA (2008). Role of mitochondria in modulation of spontaneous $Ca^{2+}$ waves in freshly dispersed interstitial cells of Cajal from the rabbit urethra. *J Physiol.* **586**, 4631–4642.

Sergeant GP, Hollywood MA, McCloskey KD, McHale NG & Thornbury KD (2001). Role of IP3 in modulation of spontaneous activity in pacemaker cells of the rabbit urethra. *Am J Physiol Cell Physiol* **280**, C1349–C1356.

Sergeant GP, Hollywood MA, McCloskey KD, Thornbury KD & McHale NG (2000). Specialised pacemaking cells in the rabbit urethra. *J Physiol* **526**, 359–366.

Sergeant GP, Hollywood MA, McHale NG & Thornbury KD (2006*b*). $Ca^{2+}$ signalling in urethral interstitial cells of Cajal. *J Physiol* **576**, 715–720.

Sergeant GP, Johnston L, McHale NG, Thornbury KD & Hollywood MA (2006*a*). Activation of cGMP/PKG pathway inhibits electrical activity in rabbit urethral interstitial cells of Cajal by reducing the spread of $Ca^{2+}$ waves. *J Physiol* **574**, 167–181.

Smith GD, Keizer JE, Stern MD, Lederer WJ & Cheng H (1998). A simple numerical model of calcium spark formation and detection in cardiac myocytes. *Biophys J* **75**, 15–32.

Terentyev D, Viatchenko-Karpinski S, Valdivia HH, Escobar AL & Gyorke S (2002). Luminal $Ca^{2+}$ controls termination and refractory behaviour of $Ca^{2+}$ induced $Ca^{2+}$ release in cardiac myocytes. *Circ Res* **91**, 414–420.

Thornbury KD, Hollywood MA, McHale NG & Sergeant GP (2011) Cajal beyond the gut: interstitial cells in the urinary system – towards general regulatory mechanisms of smooth muscle contractility? *Acta Gastro-Enterol Bel* **74**, 536–542.

Tumelty J, Scholfield CN, Stewart MT, Curtis TM & McGeown JG (2007). $Ca^{2+}$ sparks constitute elementary building blocks for global $Ca^{2+}$ signals in myocytes of retinal arterioles. *Cell Calcium* **41**, 451–466.

Wagner J & Keizer JE (1994). Effects of rapid buffers on $Ca^{2+}$ diffusion and $Ca^{2+}$ oscillations. *Biophys J* **67**, 447–456.

Ward SM, Dixon RE, deFaoite A & Sanders KM (2004). Voltage-dependent calcium entry underlies propagation of slow waves in canine gastric antrum. *J Physiol* **561**, 793–810.

Yao Y, Choi J & Parker I (1995). Quantal puffs of intracellular $Ca^{2+}$ evoked by inositol triphosphate in *Xenopus* oocytes. *J Physiol* **482**, 533–553.

Yao Y & Parker I (1994). $Ca^{2+}$ influx modulation of temporal and spatial patterns of inositol triphosphate-mediated $Ca^{2+}$ liberation in *Xenopus* oocytes. *J Physiol* **476**, 17–28.

ZhuGe R, Fogarty KE, Baker S, McCarron J, Tuft RA, Lifshitz L & Walsh JV (2004). $Ca^{2+}$ spark sites in smooth muscle cells are numerous and differ in number of ryanodine receptors, large conductance $K^+$ channels, and coupling ratio between them. *Am J Physiol Cell Physiol* **287**, C1577–C1588.

ZhuGe R, Tuft RA, Fogarty KE, Bellve K, Fay FS & Walsh JV (1999). The influence of sarcoplasmic reticulum $Ca^{2+}$ concentration on $Ca^{2+}$ sparks and spontaneous transient outward currents in single smooth muscle cells. *J Gen Physiol* **113**, 215–228.

## Additional information

### Competing interests

None declared.

### Author contributions

Conception and design of the experiments: B.T.D., G.P.S., M.A.H., K.D.T., B.J.H. and N.G.M. Collection, analysis and interpretation of data: B.T.D., G.P.S., R.J.L., K.D.T., B.J.H. and N.G.M. Drafting the article or revising it critically for important intellectual content: B.T.D., G.P.S., M.A.H., K.D.T., S.A.B., B.J.H. and N.G.M.

### Funding

This work was funded through the National Biophotonics Imaging Platform by a Higher Education Authority of Ireland PhD scholarship to B.T.D. under the HEA Programme for Research in Third Level Institutions (PRTLI) Cycle 4.

## Supporting information

The following supporting information is available in the online version of this article.

**Figure S1**
**Figure S2**